WARK-LOVERING RIMS AT THE NANOMETER SCALE: A TRANSMISSION ELECTRON MICROSCOPY STUDY. A. Toppani[1, *], J. M. Paque[2], D. S. Burnett[2], N. Teslich[1], W. Moberlychan[1], Z.R. Dai[1, *] and J. P. Bradley[1, *]. [1]LLNL, 7000, East Avenue, L-413, Livermore, CA, 94550 (toppani2@llnl.gov), [2]Califonia Institute of Technology, MS 100-23, Pasadena, CA 91125. [*] BayPac members.

Introduction: Wark-Lovering rims (WLR) consist of a sequence of mono-mineral layers a few micrometers thick (hibonite, perovskite, spinel, melilite, anorthite, pyroxene, olivine) surrounding most coarse-grained Ca-Al-rich inclusions (CAIs) [1]. Despite numerous studies, their formation is still not well understood. Based on their mineralogy [1], their rare earth element (REE) content [2] or their Mg isotopic signatures [e.g., 3], several scenarios of formation have been proposed, including (i) condensation, (ii) flash-heating and/or (iii) reaction of the CAI with a Mg-Si-rich reservoir (gaseous or solid) [e.g. 1-5]. Recent Al/Mg isotope dating suggests that formation of WLR post-dated the formation of the CAIs [6]. Finally, recent O isotopic measurements showed that minerals of the WLR have a ^{16}O enrichment similar to that of the CAI interior [7, 8], suggesting that they probably formed in the same ^{16}O rich-reservoir.

Despite their very fine-grained mineralogy (mineral layers are a few µm thick), no transmission electron microscopy (TEM) studies have been performed on WLR. This was especially due to the difficulty of preparing thin sections of specific locations of a CAI useful for mineralogical observations. In this work, we studied the mineralogy at the nanometer scale of the WLR of a CAI from the reduced CV3 chondrite Leoville. TEM sections were prepared using the Focused Ion Beam (FIB) technique [9] as it allows the observation of specific sites of an object already characterized for mineralogy, petrology or isotopic compositions. Mineralogy and chemistry at the nm to µm scale (e.g., exact chemical composition of individual sub-µm minerals, microtextures of each mineral layer or crystallographic relationships between the mineral layers) will give new information about the formation of the WLR. This should help to better understand their formation and thus the conditions that prevailed in the early solar nebula and the physical processes responsible for the first step of dust formation from the solar nebula gas.

Sample preparation: USNM 3537-2 is a coarse-grained spheroidal type B1 CAI of about 7 mm in diameter with a flat type I REE pattern [10]. It presents a fairly continuous WLR of ~ 40 to 80 µm [11]. In order to facilitate the sample preparation, a thin part of the WLR has been chosen and was studied by scanning electron microscopy (SEM) in order to be able to compare TEM and SEM results. We also chose this part as it was showing the whole mineralogical sequence and a variety of textures. The sequence consists, from the interior toward the edge, of hibonite / perovskite / melilite, spinel, anorthite, and pyroxene layers.

The thin sections of the WLR have been prepared using the 30 keV focused Gallium Ion Beam at the Lawrence Livermore National Laboratory (LLNL). Because of the large width of the WLR (~ 40 µm), a series of 4 sections has been prepared to cross the entire rim. Deposition of a 2-3 µm thick Pt-strip protecting the chosen WLR location was followed by the ion beam trenching of about 0.5-1 µm thick section. The section was then extracted from the bulk material using an in-situ method that results in the section being welded to the TEM grid using Pt [12]. Sections were then thinned in situ down to 100 nm. Under similar experimental conditions, fragile phases such as phyllosilicates, glass, or even organic material were left undamaged, suggesting that our final TEM sections were not damaged during their preparation. Four final sections were recovered from area 1 of the WLR with dimensions of about 6 micron height and 15 to 18 µm length.

Using the capacity of the new superSTEM at LLNL, precise chemical analyses (detection level down to 500 ppm), X-ray and electron energy loss mapping (high X-ray count rates using a ~1nm diameter nanoprobe), Z-contrast imaging, dark field imaging and conventional TEM work has been performed in order to characterize the WLR sections.

Results: Here, we report the study of the first three sections, namely WL-1 ext, WL-1 middle and WL-1 int. WL-1 ext is going from the matrix to the anorthite layer (matrix, pyroxene layer, anorthite layer), WL-1 middle from the pyroxene layer to the spinel layer (pyroxene, anorthite and spinel layers) and WL-1 int from the spinel layer to the hibonite/perovskite/melilite layer, respectively. Each layer was fairly homogenous and distinctive. Despite the fine-grained mineralogy of the WLR, porosity was absent. Deformation features (e.g. strain contrast) were observed throughout the WLR [13], which may be related to those observed in the meteorite.

Matrix-CAI boundary: Leoville matrix shows the presence of 100 nm to 1 micron anhydrous crystals (e.g., Fe-rich olivine (Fo 45) and enstatite, see also [13]). One very large crystal of kamacite (several µm) is standing at the contact with the WLR. Contact between the matrix and the WLR is very sharp suggesting the absence of a thermal relationship between the matrix and the WLR (Fig. 1a).

Pyroxene layer: Euhedral diopside crystals (with size around 1 µm) form a homogeneous boundary at the limit with the matrix. The euhedral diopside crystals located toward the interior of rim layer are larger in size, from 2 to 3 µm. Glass inclusions were observed in two diopside crystals sitting near the anorthite layer. Amorphous material was observed at the boundary between diopside crystals and at triple junctions between diopside crystals. Diopside crystals next to the matrix have a very low Fe content, even those in contact with the kamacite. Al and Ti contents of the pyroxene do not increase evenly toward the interior of the WLR. Indeed, both Al-Ti rich diopside (e.g. up to 12.4 wt% Al_2O_3, 3.88 wt% TiO2) and Al-Ti-poor diopside (0.48 wt% Al_2O_3, 0.09 TiO_2) were observed in contact with the anorthite layer.

Anorthite layer: Anorthite is sandwiched between pyroxene and spinel with a layer of Al-Si-Fe-rich amorphous material on both sides of the anorthite. Fe-rich crystals were found in these amorphous layers, such as a Fe-Ni-rich oxide or Fe-bearing spinels. Rounded Fe-poor spinel crystals were also observed inside the anorthite crystals.

Spinel layer: Spinels are fairly homogeneous 1 to 4 µm crystals (Fe content below detection level). While triple junctions are present, no amorphous layer was observed at the crystal boundaries. No epitaxial relationship was observed between the different spinel grains. Crystals with unusual chemical composition (28-30 wt% Al_2O_3, 25 wt% SiO_2, 23-25% CaO, 17.5 wt% TiO_2, 4.5 % MgO) were observed in several locations.

Hibonite/perovskite/melilite layer: The contact between spinel crystals (from the spinel layer) and hibonite and melilite crystals is sharp (Fig. 1c). In addition to the absence of epitaxial relationship between the spinel crystals, this contact suggests that the spinel crystallized from a liquid. Only one crystal of perovskite was observed on the edge of the section. Micrometer-sized laths (up to 5 µm) of hibonite (with up to 4 wt% MgO, 7 wt% TiO_2, 0.5 wt% SiO_2) are embedded in an Al-rich amorphous matrix with variable composition (e.g., 50 wt% Al_2O_3, 25-37 wt% SiO_2, 3-8 wt% CaO, 1-4 wt% MgO, up to 3 wt% of Fe_2O_3). A typical triple junction partly filled with amorphous material was observed at the boundary between three hibonite crystals (Fig. 1b).

Conclusion: The presence of triple junctions and amorphous material in different mineralogical layers suggests the crystallization of at least part of the WLR from a liquid. The presence of large amounts of amorphous material suggests that formation of the WLR was the last high-temperature event that occurred in the CAI life. However, some features, such as the chemical composition of the amorphous matrix in the hibonite layer are more difficult to explain in a conventional scenario of crystallization and suggest, for example, the latter interaction of this amorphous material with a more Si-Mg-rich reservoir. Because of the presence of Fe-rich phases and of the Fe content of the amorphous material, alteration (certainly pre-accretionary) of the WLR has also to be considered. Our observations ruled out the formation of the WLR by interaction of the CAI with the matrix. More interpretation will be presented at the meeting.

References: [1] Wark, D.A. and Lovering, J.F. (1977) *LPSC VIII*, 95-112. [2] Wark, D. and Boynton, W. (2001) *MAPS, 36*, 1135-1166. [3] Simon, J.I et al. (2005) *EPSL, 238*, 272-283. [4] Ruzicka, A. (1997) *JGR, 102*, 13387-13402. [5] MacPherson, G.J. (1981) *LPI XII*, 648-650. [6] Taylor, D.J. et al. (2005) *LPSC XXXVI*, # 2121. [7] Cosarinsky, M. et al. (2005) *LPSC XXXVI*, #2015. [8] Yoshitake, M. et al. (2002) *LPSC XXXIII*, #1502. [9] Heaney, J.H. et al. (2001) American Mineralogist 86, 1094-1099. [10] Sylvester, P.J. et al. (1992) GCA, 56, 1343-1363. [11] Caillet, C. et al. (1993) *GCA, 57*, 4725-4743. [12] Smith, J.B. et al. (2005) LPSC XXXVI, #1003 [13] Nakamura, T. et al. (1992) *EPSL, 114*, 159-170.

Acknowledgments: This work was performed under the auspices of the U.S. Department of Energy, National Nuclear Security Administration by the University of California, LLNL under contract No. W-7405-Eng-48. This work was supported by NASA grants NNH04AB491 (Origins) and NNH04AB521 (Cosmochemistry).

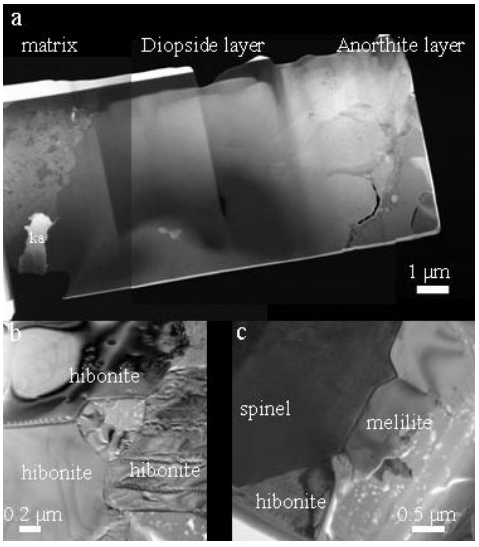

Figure 1: WLR of CAI #3537-2. a) Dark-field STEM image of WL-1 ext section (ka stands for kamacite). b and c) are bright-field TEM images from the WL-1 int section and show the triple junction between three hibonite grains and the contact between the spinel layer with the melilite/hibonite layer.